TITLE

White matter developmental trajectories associated with persistence and recovery of childhood stuttering

Ho Ming Chow[1*], Soo-Eun Chang[1]

[1]Department of Psychiatry, University of Michigan, Ann Arbor, MI

*Corresponding author

Department of Psychiatry

University of Michigan

Rachel Upjohn Building Rm 2541

4250 Plymouth Rd. Ann Arbor, MI 48109

Tel: 734-232-0300

Fax: 734-936-7868

Email: homingc@med.umich.edu

Running title: White matter development in children who stutter

This is the author manuscript accepted for publication and has undergone full peer review but has not been through the copyediting, typesetting, pagination and proofreading process, which may lead to differences between this version and the Version record. Please cite this article as doi:10.1002/hbm.23590.

ABSTRACT

Stuttering affects the fundamental human ability of fluent speech production, and can have a significant negative impact on an individual's psychosocial development. While the disorder affects about 5% of all preschool children, approximately 80% of them recover naturally within a few years of stuttering onset. The pathophysiology and neuroanatomical development trajectories associated with persistence and recovery of stuttering are still largely unknown. Here, we report the first mixed longitudinal diffusion tensor imaging (DTI) study of childhood stuttering. A total of 195 high quality DTI scans from 35 children who stutter (CWS) and 43 controls between 3-12 years of age were acquired, with an average of three scans per child, each collected approximately a year apart. Fractional anisotropy (FA), a measure reflecting white matter structural coherence, was analyzed voxel-wise to examine group and age-related differences using a linear mixed-effects (LME) model. Results showed that CWS exhibited decreased FA relative to controls in the left arcuate fasciculus, underlying the inferior parietal and posterior temporal areas, and the mid body of corpus callosum. Further, white matter developmental trajectories reflecting growth rate of these tract regions differentiated children with persistent stuttering from those who recovered from stuttering. Specifically, we found a reduction in FA growth rate (i.e., slower FA growth with age) in persistent children relative to fluent controls in the left arcuate fasciculus and corpus callosum, which was not evident in recovered children. These findings provide first glimpses into the possible neural mechanisms of onset, persistence, and recovery of childhood stuttering.

INTRODUCTION

In stuttering, frequent and involuntarily occurring sound repetitions, prolongation and blocks (abnormal stoppages) disrupt the normally effortless and rhythmic flow of speech. The typical onset of stuttering occurs between 2 and 5 years of age and affects about 5% of preschool children. Approximately 80% of children diagnosed with developmental stuttering recover naturally in early childhood – the vast majority of these recoveries occur within 2 years of stuttering onset (Bloodstein and Ratner, 2008; Yairi and Ambrose, 1999; Yairi and Ambrose, 2005) – while the other 20% continue to stutter for the rest of their lives. Persistent stuttering can have a strong negative impact on the individual's social, emotional, academic, and vocational development (Craig et al., 2009; Rees and Sabia, 2014).

The pathophysiology of stuttering is still unclear. There is, however, increasing evidence of subtle structural and functional differences in the brains of adults and children who stutter relative to their fluent peers (Beal et al., 2013; Chang et al., 2017; Chang and Zhu, 2013; Chang et al., 2015; Connally et al., 2014; Cykowski et al., 2010; Desai et al., 2016; O'Neill et al., 2017; Watkins et al., 2008). One line of research investigated the property of white matter microstructure by measuring fractional anisotropy (FA), which reflects white matter coherence or integrity, through diffusion tensor imaging (DTI). Whereas previous studies have shown that both adults and children who stutter exhibit lower FA values relative to matched controls in white matter tracts supporting speech motor control, the precise location of these differences has been inconsistent (Cai et al., 2014; Cykowski et al., 2010; Neef et al., 2015). For example, lower FA associated with stuttering has been reported along the left superior longitudinal fasciculus/arcuate fasciculus underlying the inferior frontal gyrus (BA44, Chang et al., 2015; BA47, Kell et al., 2009), premotor cortex (Chang et al., 2008; Connally et al., 2014; Watkins et

al., 2008), rolandic operculum (Chang et al., 2008; Sommer et al., 2002), and inferior parietal region (Chang et al., 2008; Chang et al., 2015; Watkins et al., 2008). FA reductions along other white matter structures such as the corticospinal tract (Cai et al., 2014) and the corpus callosum (Chang and Zhu, 2013; Chang et al., 2015; Cykowski et al., 2010) have also been reported. One recent meta-analysis of previous DTI studies of people who stutter reported convergent FA reductions associated with developmental stuttering in the arcuate fasciculus (underlying most of the frontoparietal regions reviewed above) and the body of the corpus callosum (see Fig. 1B in Neef et al., 2015).

There are many plausible reasons for the disparate locations of FA reduction found in the previous studies. For example, most of the reviewed studies published to date were based on relatively small numbers of adolescents and adults (sample sizes ranging from 13-29 people who stutter; Neef et al., 2015) and thus may lack the statistical power to distinguish an effect of a certain size from random chance. Accordingly, most studies have used a relatively lenient statistic threshold. In addition, these studies differed from one another in terms of subject demographics including age and sex composition, which likely contributed to the heterogeneity of results. Studying adults also captures the effects of adaptation and compensatory mechanisms, comorbidity, therapy, and other conditions that are associated with decades of stuttering, with varying influences across individuals. Furthermore, in the case of the few studies conducted in children who stutter, the stuttering group may have included those who eventually recover versus persist in stuttering, which may have increased variability in the findings. Additionally, since most previous studies have only examined adults or older children whose stuttering is already persistent, an important question has gone unanswered: What are the neural mechanisms underlying natural recovery of childhood stuttering?

To address these issues, we conducted a longitudinal DTI study involving a large sample of children who do and do not stutter. We investigated how developmental trajectories of white matter in persistent and recovered children who stutter deviate from typically-developing children. Characterizing these developmental trajectories is necessary not only to understand neural mechanisms linked to stuttering risk, but also to elucidate childhood neuroplasticity that leads to natural recovery from stuttering. It is crucial to identify early neural biomarkers of persistence and recovery of stuttering in order to determine targets for intervention and improve therapy.

We hypothesized that FA reductions in the tracts identified in a recent meta-analysis (Neef et al., 2015) based on previous DTI studies of persistent stuttering (i.e., arcuate fasciculus underlying frontoparietal regions and the body of the corpus callosum) are related to the risk of stuttering development and hence would be found in children who stutter, regardless of eventual outcomes of persistence or recovery. Moreover, we expected that if the FA reductions in these tracts reflect underlying stuttering behavior, there would be continued anomalous FA development in the same areas in children with persistent stuttering. Because the results from the previous DTI studies were fairly inconsistent as discussed above, we cannot however rule out the possibility of anomalous FA reduction and development in other white matter areas in children with persistent stuttering.

Recovery of stuttering may pertain to two possible scenarios. First, recovery could result from the normalization of the neural anomalies underlying the onset of stuttering. In this case, recovered children may exhibit FA values in the arcuate fasciculus and the corpus callosum that initially lag behind, but catch up later to reach comparable FA values exhibited by fluent controls. Alternatively, recovered children could exhibit an adaptive compensatory growth in

other brain areas that supports recovery from stuttering. To allow testing of this alternative hypothesis, and given the lack of existing data on the neural basis of recovery from stuttering and inconsistent results from previous DTI studies, we chose to perform a whole brain based FA analysis to examine group and age-related changes in white matter integrity in a comprehensive manner rather than restricting our analysis to specific tracts.

MATERIALS AND METHODS

Participants

Children who do and do not stutter in the 3-10 age range at initial testing were recruited for an ongoing longitudinal neuroimaging study of developmental stuttering. Each participant was scanned two to four times, with an inter-scan interval 12 months. At the time of analysis for this study, 282 DTI scans from 52 stuttering children (39 boys) and 45 controls (22 boys) were collected (age range for all visits: 3-12). Four scans (1.4%) from two participants were excluded from the analysis due to gross structural abnormalities, and another three scans (1.1%) from one participant were excluded due to poor performance (< 2 SD) on more than one standardized language tests administrated. Eighty scans (28.4%) from 51 subjects were excluded due to movement artifacts in DTI or anatomical scans (see details on exclusion criteria presented in the data analysis section). In the final analysis, 195 high quality DTI scans from 35 stuttering children (22 boys) and 43 controls (21 boys) were included. Participants' ages at the initial visit ranged from 3.2 to 10.7 years with a mean age of 6.5 and a standard deviation of 2.1 (for group specific details, see Table 1). All procedures used in this study were approved by the Michigan

State University Institutional Review Board. All children were paid a nominal remuneration, and were given small prizes (e.g., stickers) for their participation.

All participants were monolingual North American English speakers without confirmed diagnosis of developmental disorders (e.g., dyslexia, ADHD, learning delay, psychiatric conditions) other than stuttering. Details on behavioral testing procedures and a list of assessments can be found in our previous publications (Chang and Zhu, 2013; Chang et al., 2015). Briefly, each participant underwent careful screening to ensure normal speech and language development except for the presence of stuttering in the experimental group. These tests included the Peabody Picture Vocabulary Test (PPVT-3; Dunn and Dunn, 2007), Expressive Vocabulary Test (EVT-2; Williams, 2007), Goldman-Fristoe Test of Articulation (GFTA-2; Goldman, 2000), Wechsler Preschool and Primary Scale of Intelligence (WPPSI-III; for children 2:6-7:3; Wechsler, 2002), and Wechsler Abbreviated Scale of Intelligence (WASI; for children aged 7 and up; Wechsler, 1999). Children were excluded if more than one of their average scores on the above tests fell below two standard deviations (SD) of the group mean on any of these standardized assessments. The average test scores for each group are listed in Table 1.

Stuttering severity was assessed by collecting samples of spontaneous speech, elicited through storytelling and conversational tasks with a parent and a certified speech-language pathologist (SLP). These samples were video-recorded and analyzed off-line according to the procedure of the Stuttering Severity Instrument Edition 4 (SSI-4; Riley and Bakker, 2009). The SSI-4 provides a composite stuttering severity rating based on frequency and duration of disfluencies occurring in the speech sample, as well as any physical concomitants associated with moments of stuttering. To confirm reliability of the SSI-4 scores, a random subset of the

speech samples (25.5%) was rated by a second independent SLPs. The intraclass correlation coefficient calculated based on the two SLPs' ratings was 0.96, indicating high reliability.

While all children who stutter were diagnosed with stuttering during their initial visit, they were later categorized as recovered or persistent through a combination of measures acquired in subsequent visits. Specifically, a child was categorized as persistent if the SSI-4 score was higher than 10 at two consecutive follow-up visits, and the onset of stuttering had been at least 36 months prior to his most recent visit. A child was considered recovered if the composite SSI-4 score was below 10 (corresponding to "very mild" in SSI-4 severity classification) at two consecutive follow-up visits. Determination of recovered or persistent also required the consideration of percent occurrence of stuttering-like disfluencies (%SLD) in the speech sample (≥3 for persistent) as well as clinician and parental reports. Similar criteria were used to determine persistence versus recovery in stuttering children in previous studies (Yairi and Ambrose, 1999). Using these criteria, we identified 12 children who recovered, hereafter "recovered" (37 scans) and 23 children with persistent stuttering, hereafter "persistent" (55 scans) in the final data set for the analyses. For controls, the inclusion criteria included never having been diagnosed with stuttering, no family history of stuttering, lack of parental concern for their child's speech fluency, and the child's %SLD was below 3%. A total of 43 controls were included (103 scans).

MRI acquisition

All MRI scans were acquired on a GE 3T Signa® HDx MR scanner (GE Healthcare) with an 8-channel head coil. During each session, 180 T1-weighted 1-mm^3 isotropic volumetric inversion recovery fast spoiled gradient-recalled images, with CSF suppressed, were obtained to cover the

whole brain with the following parameters: time of echo = 3.8 ms, time of repetition of acquisition = 8.6 ms, time of inversion = 831 ms, repetition time of inversion = 2332 ms, flip angle = 8°, and receiver bandwidth = ±20.8 kHz.

After the T1 data acquisition, first and high-order shimming procedures were carried out to improve magnetic field homogeneity. The DTI data were acquired with a dual spin-echo echo-planar imaging sequence for 12 minutes and 6 seconds with the following parameters: 48 contiguous 2.4-mm axial slices in an interleaved order, field of view = 22 x 22 cm, matrix size = 128 x 128, number of excitations = 2, echo time = 77.5 ms, repetition time = 13.7 s, 25 diffusion-weighted volumes (one per gradient direction) with b = 1000 s/mm^2, one volume with b = 0 and parallel imaging acceleration factor = 2. One staff member sat inside the scanner room next to the child at all times to monitor the child's comfort and to ensure cooperation during scanning. During acquisition of volumetric T1-weighted scans and DTI scans, the children viewed a movie to help them stay still.

DTI data analyses

To ensure good data quality, we inspected the DTI scans using a procedure similar to "Image Scrubbing", an image censoring technique that is commonly used to remove movement artifacts from functional images (Power et al., 2012). Specifically, for each DTI scan, we estimated slice-wise volume-to-volume head movements by coregistering each volume's slices to the corresponding slices in the first volume (B_0). If head movement exceeded 1 mm in more than 20% (9 slices) of the slices in a volume, that volume was considered susceptible to movement artifacts. Any scan that contained more than 10 susceptible volumes was excluded from further analysis. Additionally, we manually inspected each scan to detect any image quality issues not

captured by the quantitative method, including signal drop-outs and image artifacts such as banding. After these procedures, the remaining 195 raw DTI scans (103 for controls, 55 for persistent and 37 for recovered) were processed using Tortoise developed by the NIH Pediatric Neuroimaging Diffusion Tensor MRI Center (Pierpaoli et al., 2010). We used the "DIFF PREP" module of Tortoise to correct for image artifacts including motion, eddy-current distortion, EPI B_0 and concomitant field distortions. Diffusion tensors at each voxel were estimated using the iRESTORE algorithm implemented in the "DIFF CALC" module of Tortoise (Chang et al., 2012), and individual FA maps were output for statistical analyses. To normalize the FA maps into standard space, we first normalized individual T1-weighted anatomical images using diffeomorphic image registration algorithm (DARTEL; Ashburner, 2007) implemented in SPM12 (http://www.fil.ion.ucl.ac.uk/spm/software/spm12/). Each individual T1 image was first aligned with the DTI B_0 image. The DARTEL algorithm then segmented each T1 image into distinct tissue compartments including gray and white matter using the unified segmentation algorithm (Ashburner and Friston, 2005). Gray and white matter images of all participants were used to create a customized template. DARTEL then iteratively refined warping parameters for transforming individual subject space to the customized template, and then transformed the images from the customized template space to a standard space (ICBM152). This two-step procedure is more robust in dealing with variations of brain sizes and morphometry than normalizing brain images directly to the standard space (Yoon et al., 2009). Moreover, recent studies have shown normalizing the anatomical images of children (4 to 11 years of age) to a common space does not introduce age-related bias (Burgund et al., 2002; Ghosh et al., 2010). The individual FA maps were transformed to the standard space by applying the deformation

fields generated from DARTEL, resampled to 1.5 mm isotropic voxel size and spatially smoothed with a 4 mm FWHM Gaussian kernel.

The normalized FA maps were analyzed using a voxel-based approach. To reduce the potential effect of misalignment among participants, gray matter and gray/white boundaries were excluded using two criteria. First, voxel-wise mean FA across subjects was calculated, and voxels with mean FA less than 0.25 were excluded. Second, mean white matter probability was calculated using individual white matter maps generated in the segmentation step, and voxels with mean probability less than 0.85 were excluded. A linear mixed-effects (LME) model was used to analyze group and age-related effects on FA. LME modeling is a flexible statistical framework for analyzing longitudinal data and provides many attractive features over other methods such as repeated measures ANOVA (Bernal-Rusiel et al., 2013; Cnaan et al., 1997; Fitzmaurice et al., 2008; Pinheiro, 2005; Verbeke and Molenberghs, 2009). Specifically, LME analysis models the covariance structure of correlated data (e.g., repeated measures and longitudinal data) and is able to handle an unequal number of within-subject measurements and measurements that were recorded at the different time points across subjects, i.e., unbalanced data (Bernal-Rusiel et al., 2013; Chen et al., 2013). These advantages are particularly important to the current study because DTI scans were excluded due to severe head motion or attrition, leading to an unbalanced number of observations. LME modeling has been used in longitudinal studies that are similar in design to the current study; LME modeling was used to examine developmental trajectories of cortical thickness and volume associated with autism (Lange et al., 2015; Schumann et al., 2010; Zielinski et al., 2014) and intellectual ability (Shaw et al., 2006). Our effects of interest were modeled as fixed-effects (i.e., explanatory variables) and included group (control, persistent, recovered) and group by age interactions. Additionally, subject was

included as a random-effect to account for within-subject variability. Our model also included socioeconomic status, IQ, sex, group-by-quadratic-age interactions, and the head motion measure as fixed-effects to capture effects of no interest. Although IQ, PPVT, and EVT scores were significantly lower in the persistent group relative to controls, we only included IQ in the LME model because these three measures were highly correlated ($r > 0.7$). Stuttering severity as measured by SSI-4 was not included in the model because it was used to define persistent and recovered groups, but the relation between FA and stuttering severity in children with persistent stuttering was examined in separate analysis. Voxel-wise LME models were estimated using the fitlme function in Matlab (Release 2013b, The Mathworks Inc., Natick, Massachusetts). T-tests were used to compare model estimates between groups. False positives due to multiple testing were controlled by a combination of *p*-value and a spatial extent (cluster size) threshold (*k*). The cluster size threshold was estimated using the recommended procedure of AFNI 3dClustSim (March 2016 version; http://afni.nimh.nih.gov/pub/dist/doc/program_help/3dClustSim.html). Unless otherwise specified, the thresholds were set at $p<0.01$ and $k>33$ voxels, corresponding to a corrected *p*-value of 0.05.

A more common approach used to localize white matter group differences is tract-based spatial statistics (TBSS). This method aims to reduce inter-subject misalignment errors by projecting FA values to a pseudo-anatomical white matter skeleton (Smith et al., 2006). Although TBSS may reduce misalignment errors by up to 10%, it is less sensitive to FA abnormalities that occur further away from the skeleton and may therefore sacrifice potentially important anatomical information (Zalesky, 2011). Indeed, a recent study has shown that the benefits of using TBSS diminish, and a voxel-based approach outperforms TBSS, when a superior non-linear coregistration algorithm similar to the one adopted in the current study was

used (Schwarz et al., 2014). By using this approach, we were able to acquire more precise anatomical specificity of white matter group differences. Nevertheless, we also carried out a TBSS analysis to confirm that our results were not due to inter-subject misalignment and to provide a more direct comparison with previous studies using TBSS. We used FSL's Diffusion Toolbox to carry out TBSS projection with the default settings. Specifically, FA values greater than 0.2 in the normalized, unsmoothed individual images were projected to the TBSS skeleton. The same LME model as in the voxel-based analysis was used to estimate FA differences between groups. For the TBSS analysis, statistical threshold was set at $p<0.005$ (uncorrected). This threshold is similar to the statistical thresholds used in other TBSS studies on stuttering (Cai et al., 2014; Chang et al., 2015; Connally et al., 2014). Importantly, we found high correspondence between the voxel-based and TBSS analyses; 56 out of 64 (87.5%) clusters identified in the voxel-based analyses spatially overlapped with a significant cluster in the same TBSS analyses. In this study, only those clusters with overlap between the voxel-based and TBSS analyses are reported. The corresponding TBSS results are presented in the supplementary materials (Tables S1 and S2).

To illustrate the white matter tracts associated with FA group differences, we performed fiber tracking on the DTI data of a 9-year-old female subject who had minimal head movements during scanning using the deterministic tractography algorithm implemented in TrackVis (Wang et al., 2007). An angle threshold of 45° was applied to prevent abrupt change of fiber orientation during the tracking process. Furthermore, white matter areas exhibiting significant group differences, we extracted and averaged the individual model estimates of group and age plus residuals and random intercepts (i.e., raw FA values minus effects of no interests) from voxels within a 5 mm radius sphere centered at the peak coordinates of each cluster significant based on

the between-group contrast. FA values of each group were plotted against participants' chronological age.

To further explore whether an association exists between FA and stuttering severity as measured by SSI-4, we conducted two analyses. Because severity scores of children who recovered at the follow-up visits were very low (<10), the relation between FA and severity may not be very clinically meaningful. Moreover, the fluency of children who recover from stuttering improved over time, as it was the definition of recovery in the current study. Thus, stuttering severity may be confounded with an age-related effect. Therefore, we focused on data from children with persistent stuttering to examine the association between stuttering severity and FA. We first used a region of interest approach to examine whether FA in the regions exhibiting a significant group or group-by-age difference in children with persistent stuttering relative to controls was associated with stuttering severity. Based on the results of the main analyses, the peak coordinates of each region were identified, and FA within 5 mm of each coordinate was extracted and averaged. The same LME model as the main analyses was used to examine the association between FA and severity, except that SSI-4 scores were added as a fixed effect, and the effects of control and recovered groups were removed. A false discovery rate method was used to correct for multiple comparisons due to the number of regions selected. To further explore if there was a relation between stuttering severity and FA in the white matter areas in which no significant group or group-by-age differences were detected, the same LME analysis was repeated for all of the voxels in the whole brain. For this whole-brain analysis, we applied the same threshold as in the main analyses.

RESULTS

Participant characteristics

The groups of children with persistent stuttering ("persistent"), those recovered from stuttering ("recovered"), and fluent controls did not differ significantly in mean age, inter-scan interval, average number of scans, socioeconomic status, or sex ratios (Table 1). There was no significant difference among subject groups in the proportions of children scanned at each 2-year age bracket [$\chi 2$ (8, N=195)=7.36, p=0.50], nor in the proportions of first-visit scans acquired at each bracket [$\chi 2$ (6, N=78)=2.27, p=0.89]. The number of scans by age bracket in each group can be found in the supplementary materials (Table S3). Compared to controls, children with persistent stuttering scored significantly lower on IQ, PPVT, and EVT (p<0.05; Table 1), while recovered children only scored lower on IQ and EVT (p<0.05; Table 1). Persistent and recovered groups did not differ significantly on any of the standardized tests, nor in stuttering severity at initial visit. As expected, the difference in stuttering severity became highly significant based on measurements acquired at their last visits (p<0.01), indicating the divergence of symptoms between the persistent and recovered groups with progressing age.

FA deviations from controls associated with persistence and recovery of stuttering (between-group differences)

Compared to controls, both persistent and recovered groups exhibited FA reductions in the left arcuate fasciculus in the inferior parietal lobule (i.e., a part of the superior longitudinal fasciculus) as well as in the posterior temporal lobe (Fig. 1A, and scatter plots in Fig. 1C). Another set of FA reductions for both stuttering groups relative to controls was found in the corpus callosum, which contains tracts that interconnect the bilateral motor cortical regions (Fig.

1B & 1C). Compared to controls, the persistent group showed a reduction in the mid-section of the corpus callosum body and splenium whereas recovered children showed FA reductions in the superior part of the corpus callosum body, near the supplementary motor area (SMA) (Fig. 1B & 1C). In addition to these FA reductions, increased FA was observed in the superior part of the corpus callosum body for the persistent group relative to controls. The details of the white matter regions showing significant group differences can be found in Table 2.

Unique white matter developmental trajectories associated with persistence and recovery of stuttering (group by age interactions)

Compared to controls, the FA growth rate of persistent but not recovered children was lower in both parietal and temporal parts of the left arcuate fasciculus (Fig. 2A, and scatter plots in Fig. 2E) as well as the parietal part of the right arcuate fasciculus. The scatter plots in Fig. 2E show that in the left arcuate fasciculus, FA of both control and recovered groups increased with age whereas FA of the persistent group decreased with age. Additionally, the persistent group showed a lower FA growth rate in mid-line white matter structures including the body of corpus callosum, cingulum, superior thalamic radiation (Fig. 2B & 2E), anterior thalamic radiation (Fig. 2C & 2E), and the cerebral and cerebellar peduncles (Fig 2D & 2E). An anterior area that exhibited a lower FA growth rate in the persistent group (cluster 9 in Fig. 2C & 2E) was related to the anatomical connections of the inferior frontal gyrus. While the recovered group also showed a lower FA growth rate in the body of corpus callosum and the anterior thalamic radiation, the spatial extent was much smaller than that exhibited by the persistent group (Fig. 2B & 2E). Unique to the recovered group, a lower FA growth rate was found in the right inferior longitudinal fasciculus (anterior temporal part) and the left dorsolateral frontal area when compared to controls (Table 3).

Compared to controls, a higher FA growth rate was found in some areas for both stuttering groups. For children with persistent stuttering, a higher FA growth rate was found in the splenium of the corpus callosum, but for recovered children, a higher FA growth rate was observed in the body of corpus callosum near the SMA and the cerebellum (Table 3).

Relation between stuttering severity and white matter development

The relation between FA and stuttering severity of children with persistent stuttering were examined using both regions of interest and whole-brain approaches. For the region of interest analysis, based on the main analyses between persistent and control groups, 24 regions were identified (see Table 1 and 2). FA was analyzed using the same LME model for the main analyses, except the SSI-4 scores were added as a fixed effect. No significant effect of stuttering severity was found for any of the regions selected after correcting for multiple comparisons. Even when an uncorrected threshold of $p<0.05$ was used, the effect of stuttering severity in most of the regions was not significant. For the whole brain analysis, the same LME model was used. A significant negative relation between FA and severity was found in three clusters located in the anterior and superior thalamic radiations (see Table 4).

DISCUSSION

We investigated how developmental trajectories of white matter in children with persistent stuttering and those recovered from stuttering deviate from typically developing children in early to late childhood. Our results demonstrated that the risk of stuttering, regardless of eventual persistence or recovery, was associated with overall FA reductions in parietal-temporal areas of the left arcuate fasciculus and the body of the corpus callosum. Furthermore, stuttering

persistence was specifically associated with reduction of growth rate in white matter tracts interconnecting the left frontotemporal regions, bilateral motor areas and the basal ganglia. We first discuss findings related to significant group differences in FA, followed by age-related differences that provide novel insights on the interaction between development and stuttering that may affect eventual persistence or recovery.

White matter group differences that characterize persistence and recovery of stuttering

The main group comparisons revealed a reduction of FA in the inferior parietal and posterior temporal parts of the left arcuate fasciculus in children who stutter, consistent with previous work (Chang et al., 2008; Chang et al., 2015) and findings from the recent meta-analysis of DTI studies on stuttering (Neef et al., 2015). Children with persistent stuttering also exhibited FA reduction in the body and splenium of the corpus callosum similar to what has been found in adults who stutter (Connally et al., 2014; Cykowski et al., 2010). However, some previously reported FA reductions were not observed. For example, FA reductions were not found in frontal speech motor areas such as the inferior frontal gyrus (IFG) (Chang et al., 2015; Kell et al., 2009), cerebellar peduncles (Connally et al., 2014; Watkins et al., 2008), and the genu of the corpus callosum (Civier et al., 2015; Cykowski et al., 2010) in children with persistent stuttering relative to controls. Instead, children with persistent stuttering exhibited lower FA *growth rate* when compared with controls (i.e., age by group interaction) in those tracts. This suggests that the reduction of FA in the IFG, the cerebellar peduncles, and the genu of the corpus callosum observed in adults who stutter may present gradually during childhood and adolescence.

To date, only one other DTI study has investigated white matter anomalies in children who recovered from stuttering (Chang et al., 2008), and did not find any statistically significant

difference in FA between groups, likely due to lack of statistical power. However, with a larger sample, we found the pattern of FA reductions between the recovered and control groups was surprisingly similar to the pattern observed when comparing persistent and control groups. Relative to controls, both persistent and recovered groups exhibited FA reductions in the parietal and posterior temporal parts of the left arcuate fasciculus as well as the body of the corpus callosum. Although the location of FA reductions in the commissural fibers were different in the two stuttering groups (i.e., closer to the mid-section for persistent, but beneath the SMA for recovered), both locations likely affect interhemispheric connections of motor areas and contribute to the risk of stuttering regardless of eventual persistence or recovery.

White matter developmental trajectories that differentiate persistence and recovery of stuttering

The analysis of group by age interactions showed that children with persistent stuttering exhibit a distinct pattern of FA development compared to controls and children who recovered. In contrast to a general increase of FA with age in the control and recovered groups, the persistent group exhibited a reduction of FA with age in the same white matter tracts (i.e., the left arcuate fasciculus and the body of the corpus callosum). Additionally, children with persistent stuttering exhibited a reduction of FA growth rate in the motor pathways as well as connections between prefrontal areas. A reduction of FA growth rate in the body of the corpus callosum was also found in recovered children, but this was less prominent relative to persistent children. The anomalous FA growth rate in the tracts noted above may impede adaptation processes that could otherwise compensate for the deficits associated with the risk of stuttering. This interpretation is further elaborated in the context of recent theories of stuttering in the next section.

Implications on neuroanatomical theories of stuttering

According to an influential neuro-computational model of speech, three interactive components are critical for fluent speech production (Civier et al., 2013; Tourville and Guenther, 2011). The first component involves the conversion of sound representations of the intended utterances to their corresponding motor representations or speech sounds. This is achieved by the interactions between the posterior temporal, inferior frontal and the ventral premotor areas (Hickok et al., 2011). Second, speech sounds are only meaningful if they are produced in the correct temporal sequence. Accumulating evidence indicates that this process involves the supplementary motor and premotor areas, and the basal-ganglia-thalamocortical (BGTC) loops. The outputs of the BGTC loops project back to the cortical motor areas, generating feedforward motor commands to control motor execution and an expectation of somatosensory consequences (Alm, 2004; Civier et al., 2013; Etchell et al., 2014). The third component is the process of controlling and monitoring speech output. This is achieved via feedforward and feedback control (Perkell, 2012). Feedforward control relies on the expectation of somatosensory consequences generated from the sequencing process to control and execute speech movements. Operating in parallel with feedforward control, feedback control is accomplished by detecting discrepancies between expected and actual auditory and somatosensory consequences. This information is fed back to the BGTC loops to modify motor commands as necessary.

The core deficits of stuttering may lie among these aforementioned components. Our results provide support for aspects of those theories discussed above as FA reductions were found in the white matter tracts connecting frontotemporal regions and bilateral SMA. These anomalies may lead to generation of aberrant motor commands and expectations. As a result, the basis for feedforward control of speech cannot be established accurately. Since the feedforward

control is unreliable, children who stutter may rely more on feedback control (Civier et al., 2010; Namasivayam et al., 2009) and vacillate between the feedforward and feedback subsystems to generate speech. However, relying on feedback of the speech signal is inefficient because it is inherently delayed in time (Levelt, 1993). Thus, switching between feedforward and feedback control may interrupt continuous speech and manifest as moments of stuttering.

Interestingly, reductions of FA in the white matter tracts connecting frontotemporal regions and the bilateral SMA were found in both recovered and persistent children and hence may not necessarily lead to persistent stuttering. What differentiates persistence from recovery of stuttering seems to be the *developmental trajectories*, or *growth rate*, of white matter tracts. For children who recovered from stuttering, the developmental trajectories of white matter tracts were relatively normal, suggesting the deficits associated with the risk of stuttering may be overcome in later stages of childhood. On the contrary, the growth rate of the white matter tracts connecting frontotemporal and motor regions, including the arcuate fasciculus, tracts interconnecting BGTC areas, the body of the corpus callosum and the superior thalamic radiations, were anomalous in children with persistent stuttering. These developmental trends may further exacerbate aberrant feedforward control, and anomalous integration of the two hemispheres to support speech movements in the persistent group. Moreover, children with persistent stuttering exhibited an anomalous reduction of white matter growth rate in the cerebral and cerebellar peduncles that connect the cortical motor areas to the lower motor neurons and the cerebellum respectively. This age-related difference between persistent stuttering and control groups were also previously reported in adults (Connally et al., 2014). Atypical development in these tracts is likely to affect motor control and execution, consistent with the empirical findings that have shown relatively unstable speech timing and coordination of articulatory movements of

adults and children who stutter (Smith et al., 2012; Smith et al., 2010; Walsh et al., 2015). These instabilities in speech output may affect the optimization of feedforward control since a stable reference from feedback is missing (Perkell, 2012).

Another area in which persistent children exhibited a decrease in FA growth rate was near a junction of a number of white matter tracts that inter-connect among areas in the prefrontal cortex, including the inferior frontal gyrus. The affected tracts near the prefrontal areas include the genu of the corpus callosum that connects the bilateral IFG, the frontal aslant tract that connects the IFG and the motor areas including the SMA and pre-SMA, and the short frontal fibers that connect the IFG with other prefrontal areas (Catani et al., 2012). Due to the limitations of DTI tractography techniques, we could not confidently separate the tracts that were affected in this prefrontal region. However, all of these tracts are proximal to anatomical connections involving the IFG, and subtle deficit in this region may disrupt sound-to-motor conversion to achieve feedforward control.

Another tract related to decreased FA growth rate in persistent children was the anterior thalamic radiation, which may connect the prefrontal areas with the BGTC loops (Alexander and Crutcher, 1990; Helie et al., 2015). Although the role of this circuit in speech production is not fully understood, it has been implicated in higher-order cognitive functions, including sequence learning (Graybiel, 2005), rule-based categorization (Ashby and Maddox, 2011; Ell et al., 2010), attention switching (Ravizza and Ciranni, 2002), and working memory (Taylor and Taylor, 2000; Voytek and Knight, 2010). These functions are not only necessary for fluent speech, but are also essential for language acquisition (Friederici, 2006). We postulate that the anomalies in the connections between prefrontal areas and the basal ganglia may affect higher-order cognitive functions (e.g., attention) necessary to develop speech control automaticity (i.e., feedforward

control) through the feedback of speech outputs. This interpretation is also relevant to the current results that showed a negative relationship between stuttering severity and FA along the anterior and superior thalamic radiations in the persistent group. Specifically, lower FA in these tracts was associated with more severe stuttering in children with persistent stuttering. These results suggest that attenuated FA in tracts interconnecting frontal areas and the BGTC loops, which help interface speech motor control and other cognitive functions, may contribute to severity and persistence in stuttering.

Increased FA associated with stuttering persistence and recovery

In addition to FA reductions, we also found increased FA and higher FA growth rate in some areas in both recovered and persistent groups relative to controls. Interestingly, many of these increases were located in the nearby areas in which FA or FA growth rate was reduced for the stuttering groups. There are at least three possible explanations for this observation. First, both increases and decreases of FA relative to controls reflect dysfunction of the associated tracts. For example, increased FA in the external capsule and the basal ganglia is associated with Tourette syndrome (Thomalla et al., 2009) and Huntington's disease (Douaud et al., 2009), respectively. Second, FA increases may reflect the result of a compensatory neuroplasticity process by which alternative anatomical connections are developed to bypass the compromised regions or connections. Our results seem to provide support for this possibility. For example, in recovered children, an increase in FA growth rate in the body of corpus callosum near the SMA may compensate for the effect of FA reductions in the same region. Third, FA increases in one tract may be caused by FA decreases in another tract at the junction where the two tracts crossed. In this case, these FA increases are not directly related to the actual physiological changes.

Although the causes of FA increases cannot be determined easily, they are likely to be directly or indirectly related the structural anomalies underlying stuttering.

Caveats

Controlling for motion artifacts was particularly important for the current study because pediatric participants tend to move more during scanning, and motion artifacts can lead to spurious group differences in FA (Yendiki et al., 2014). To reduce the chance of obtaining spurious results due to head motions, several measures were implemented in different stages of data processing in this study. First, we excluded approximately one third of the scans that were susceptible to extensive image corruption due to motion artifacts using a quantitative method. Second, diffusion tensor was estimated using iRESTORE algorithm, which has been shown to be able to accurately estimate diffusion tensors even though around 17% of the gradient directions in the data were corrupted by physiological and motion artifacts (Chang et al., 2012; Liu et al., 2015). Third, we included the movement measure in the statistical model as a nuisance regressor as suggested in Yendiki et al. (2014). Although the adverse effect of head motions cannot be ruled out completely, we believe that these conservative measures have minimized possible spurious results caused by motion artifacts.

The sample size of current study is the largest pediatric DTI data set in the field to date. However, the sample size of children who recovered from stuttering was relatively small (12 participants and 32 scans) after removing potential corrupted DTI images using the above discussed procedures. There is a chance that heterogeneity in the population of the children who recovered from stuttering (e.g., sub-groups) may be higher than what our sample represents. Hence, the results should be interpreted with caution. Moreover, the developmental trajectories

presented in this study should be interpreted as overall trends, and are not presently applicable to a specific, narrower age range (e.g., preschool age). More data and additional analyses are needed to examine finer-grained differences in various age groups.

In the current study, we used DTI tractography of a single participant to illustrate the white matter tracts that are potentially affected by FA anomalies identified in our analyses. These illustrations are solely intended to assist the reader to visualize the anatomical connections, but they could be anatomically imprecise for several reasons. First, although the tractography results obtained from the participant we selected seem to be consistent with established anatomical connections according to different sources of evidence, including DTI (e.g., Mori et al., 2005) and animal tracing studies (Schmahmann and Pandya, 2009), there are natural variations among participants and thus the tractography results cannot be generalized. Second, most DTI tractography techniques cannot effectively separate crossing fibers, leading to stoppages of tract tracing at tract junctions. Due to these limitations, tract-related interpretations should be primarily based on the locations of FA anomalies and our understanding of anatomical connections obtained from previous studies.

Conclusion

This study provides the first evidence that children with persistent stuttering have different trajectories of white matter development relative to children who recover from stuttering. Moreover, the current study showed that regardless of eventual recovery or persistence, stuttering is associated with an overall decrease in FA in both the left arcuate fasciculus and the corpus callosum, suggesting that the anomalies in these two tracts are associated with risk of childhood onset stuttering. However, there was a marked difference between persistent and

recovered groups in FA developmental trajectories. Children with persistent stuttering showed an anomalous growth in white matter tracts inter-connecting the speech motor areas, but children who recovered showed relatively normal development in these same tracts. These results point to normal (though delayed) developmental trajectories of white matter tracts in recovered children that eventually can adequately support fluent speech production, but a persisting anomalous developmental trajectory in children who continue to stutter. Further investigation is needed to understand the factors and mechanisms driving these developmental changes that may help develop treatment strategies to mitigate stuttering symptoms and enhance chances of recovery in children who stutter.

ACKNOWLEDGEMENTS

The authors wish to thank all the children and parents who participated in this study. We also thank Kristin Hicks for her assistance in participant recruitment, behavioral testing, and help with MRI data collection, Scarlett Doyle for her assistance in MRI data acquisition, Ashley Larva for her assistance in speech data analyses, and Mike Angstadt, Ai Leen Choo, Andrew Etchell, Emily Garnett, and Daniel Kessler for their inspiring discussion.

This study was supported by Award Number R01DC011277 from the National Institute on Deafness and other Communication Disorders (NIDCD) to SC and the Matthew Smith Stuttering Research Fund to SC. The content is solely the responsibility of the authors and does not necessarily represent the official views of the NIDCD or the National Institutes of Health.

REFERENCES

Alexander GE, Crutcher MD (1990): Functional architecture of basal ganglia circuits: neural substrates of parallel processing. Trends in neurosciences, 13:266-71.

Alm PA (2004): Stuttering and the basal ganglia circuits: a critical review of possible relations. Journal of communication disorders, 37:325-69.

Ashburner J (2007): A fast diffeomorphic image registration algorithm. NeuroImage, 38:95-113.

Ashburner J, Friston KJ (2005): Unified segmentation. NeuroImage, 26:839-51.

Ashby FG, Maddox WT (2011): Human category learning 2.0. Annals of the New York Academy of Sciences, 1224:147-61.

Beal DS, Gracco VL, Brettschneider J, Kroll RM, De Nil LF (2013): A voxel-based morphometry (VBM) analysis of regional grey and white matter volume abnormalities within the speech production network of children who stutter. Cortex; a journal devoted to the study of the nervous system and behavior, 49:2151-61.

Bernal-Rusiel JL, Greve DN, Reuter M, Fischl B, Sabuncu MR, Alzheimer's Disease Neuroimaging I (2013): Statistical analysis of longitudinal neuroimage data with Linear Mixed Effects models. NeuroImage, 66:249-60.

Bloodstein O, Ratner NB (2008): A handbook on stuttering. Clifton Park, NY. Thomson Delmar Learning. xiii, 552 p. p.

Burgund ED, Kang HC, Kelly JE, Buckner RL, Snyder AZ, Petersen SE, Schlaggar BL (2002): The feasibility of a common stereotactic space for children and adults in fMRI studies of development. NeuroImage, 17:184-200.

Cai S, Tourville JA, Beal DS, Perkell JS, Guenther FH, Ghosh SS (2014): Diffusion imaging of cerebral white matter in persons who stutter: evidence for network-level anomalies. Frontiers in human neuroscience, 8:54.

Catani M, Dell'acqua F, Vergani F, Malik F, Hodge H, Roy P, Valabregue R, Thiebaut de Schotten M (2012): Short frontal lobe connections of the human brain. Cortex; a journal devoted to the study of the nervous system and behavior, 48:273-91.

Chang LC, Walker L, Pierpaoli C (2012): Informed RESTORE: A method for robust estimation of diffusion tensor from low redundancy datasets in the presence of physiological noise artifacts. Magnetic resonance in medicine, 68:1654-63.

Chang S-E, Angstadt M, Chow HM, Etchell AC, Garnett EO, Choo AL, Kessler D, Welsh RC, Sripada C (2017): Anomalous network architecture of the resting brain in children who stutter. Journal of fluency disorders.

Chang SE, Erickson KI, Ambrose NG, Hasegawa-Johnson MA, Ludlow CL (2008): Brain anatomy differences in childhood stuttering. NeuroImage, 39:1333-44.

Chang SE, Zhu DC (2013): Neural network connectivity differences in children who stutter. Brain : a journal of neurology, 136:3709-26.

Chang SE, Zhu DC, Choo AL, Angstadt M (2015): White matter neuroanatomical differences in young children who stutter. Brain : a journal of neurology, 138:694-711.

Chen G, Saad ZS, Britton JC, Pine DS, Cox RW (2013): Linear mixed-effects modeling approach to FMRI group analysis. NeuroImage, 73:176-90.

Civier O, Bullock D, Max L, Guenther FH (2013): Computational modeling of stuttering caused by impairments in a basal ganglia thalamo-cortical circuit involved in syllable selection and initiation. Brain and language, 126:263-78.

Civier O, Kronfeld-Duenias V, Amir O, Ezrati-Vinacour R, Ben-Shachar M (2015): Reduced fractional anisotropy in the anterior corpus callosum is associated with reduced speech fluency in persistent developmental stuttering. Brain and language, 143:20-31.

Civier O, Tasko SM, Guenther FH (2010): Overreliance on auditory feedback may lead to sound/syllable repetitions: simulations of stuttering and fluency-inducing conditions with a neural model of speech production. Journal of fluency disorders, 35:246-79.

Cnaan A, Laird NM, Slasor P (1997): Using the general linear mixed model to analyse unbalanced repeated measures and longitudinal data. Statistics in medicine, 16:2349-80.

Connally EL, Ward D, Howell P, Watkins KE (2014): Disrupted white matter in language and motor tracts in developmental stuttering. Brain and language, 131:25-35.

Craig A, Blumgart E, Tran Y (2009): The impact of stuttering on the quality of life in adults who stutter. Journal of fluency disorders, 34:61-71.

Cykowski MD, Fox PT, Ingham RJ, Ingham JC, Robin DA (2010): A study of the reproducibility and etiology of diffusion anisotropy differences in developmental stuttering: a potential role for impaired myelination. NeuroImage, 52:1495-504.

Desai J, Huo Y, Wang Z, Bansal R, Williams SC, Lythgoe D, Zelaya FO, Peterson BS (2016): Reduced perfusion in Broca's area in developmental stuttering. Human brain mapping.

Douaud G, Behrens TE, Poupon C, Cointepas Y, Jbabdi S, Gaura V, Golestani N, Krystkowiak P, Verny C, Damier P, Bachoud-Levi AC, Hantraye P, Remy P (2009): In vivo evidence for the selective subcortical degeneration in Huntington's disease. NeuroImage, 46:958-66.

Dunn DM, Dunn LM (2007): Peabody picture vocabulary test: Manual. Pearson.

Ell SW, Weinstein A, Ivry RB (2010): Rule-based categorization deficits in focal basal ganglia lesion and Parkinson's disease patients. Neuropsychologia, 48:2974-86.

Etchell AC, Johnson BW, Sowman PF (2014): Behavioral and multimodal neuroimaging evidence for a deficit in brain timing networks in stuttering: a hypothesis and theory. Frontiers in human neuroscience, 8:467.

Fitzmaurice G, Davidian M, Verbeke G, Molenberghs G (2008): Longitudinal data analysis. CRC Press.

Friederici AD (2006): What's in control of language? Nature neuroscience, 9:991-2.

Ghosh SS, Kakunoori S, Augustinack J, Nieto-Castanon A, Kovelman I, Gaab N, Christodoulou JA, Triantafyllou C, Gabrieli JD, Fischl B (2010): Evaluating the validity of volume-based and surface-based brain image registration for developmental cognitive neuroscience studies in children 4 to 11 years of age. NeuroImage, 53:85-93.

Goldman R (2000): Fristoe M. Goldman-Fristoe test of articulation, 2.

Graybiel AM (2005): The basal ganglia: learning new tricks and loving it. Current opinion in neurobiology, 15:638-44.

Helie S, Ell SW, Ashby FG (2015): Learning robust cortico-cortical associations with the basal ganglia: an integrative review. Cortex; a journal devoted to the study of the nervous system and behavior, 64:123-35.

Hickok G, Houde J, Rong F (2011): Sensorimotor integration in speech processing: computational basis and neural organization. Neuron, 69:407-22.

Kell CA, Neumann K, von Kriegstein K, Posenenske C, von Gudenberg AW, Euler H, Giraud AL (2009): How the brain repairs stuttering. Brain : a journal of neurology, 132:2747-60.

Lange N, Travers BG, Bigler ED, Prigge MB, Froehlich AL, Nielsen JA, Cariello AN, Zielinski BA, Anderson JS, Fletcher PT, Alexander AA, Lainhart JE (2015): Longitudinal volumetric brain changes in autism spectrum disorder ages 6-35 years. Autism research : official journal of the International Society for Autism Research, 8:82-93.

Levelt WJ (1993): Speaking: From intention to articulation. MIT press.

Liu B, Zhu T, Zhong J (2015): Comparison of quality control software tools for diffusion tensor imaging. Magnetic resonance imaging, 33:276-85.

Mori S, Wakana S, Van Zijl PC, Nagae-Poetscher LM (2005): MRI atlas of human white matter. Elsevier..

Namasivayam AK, van Lieshout P, McIlroy WE, De Nil L (2009): Sensory feedback dependence hypothesis in persons who stutter. Human movement science, 28:688-707.

Neef NE, Anwander A, Friederici AD (2015): The Neurobiological Grounding of Persistent Stuttering: from Structure to Function. Current neurology and neuroscience reports, 15:63.

O'Neill J, Dong Z, Bansal R, Ivanov I, Hao X, Desai J, Pozzi E, Peterson BS (2017): Proton Chemical Shift Imaging of the Brain in Pediatric and Adult Developmental Stuttering. JAMA psychiatry, 74:85-94.

Perkell JS (2012): Movement goals and feedback and feedforward control mechanisms in speech production. Journal of neurolinguistics, 25:382-407.

Pierpaoli C, Walker L, Irfanoglu M, Barnett A, Basser P, Chang L, Koay C, Pajevic S, Rohde G, Sarlls J (2010): TORTOISE: an integrated software package for processing of diffusion MRI data. Book TORTOISE: an Integrated Software Package for Processing of Diffusion MRI Data (Editor ed^ eds), 18:1597.

Pinheiro JC (2005): Linear mixed effects models for longitudinal data. Encyclopedia of Biostatistics.

Power JD, Barnes KA, Snyder AZ, Schlaggar BL, Petersen SE (2012): Spurious but systematic correlations in functional connectivity MRI networks arise from subject motion. NeuroImage, 59:2142-54.

Ravizza SM, Ciranni MA (2002): Contributions of the prefrontal cortex and basal ganglia to set shifting. Journal of cognitive neuroscience, 14:472-83.

Rees DI, Sabia JJ (2014): The kid's speech: The effect of stuttering on human capital acquisition. Econ Educ Rev, 38:76-88.

Riley GD, Bakker K (2009): Stuttering Severity Instrument: SSI-4. Pro-Ed.

Schmahmann JD, Pandya D (2009): Fiber pathways of the brain. OUP USA.Schumann CM, Bloss CS, Barnes CC, Wideman GM, Carper RA, Akshoomoff N, Pierce K, Hagler D, Schork N, Lord C, Courchesne E (2010): Longitudinal magnetic resonance imaging study of cortical development through early childhood in autism. The Journal of neuroscience : the official journal of the Society for Neuroscience, 30:4419-27.

Schwarz CG, Reid RI, Gunter JL, Senjem ML, Przybelski SA, Zuk SM, Whitwell JL, Vemuri P, Josephs KA, Kantarci K, Thompson PM, Petersen RC, Jack CR, Jr., Alzheimer's Disease Neuroimaging I (2014): Improved DTI registration allows voxel-based analysis that outperforms tract-based spatial statistics. NeuroImage, 94:65-78.

Shaw P, Greenstein D, Lerch J, Clasen L, Lenroot R, Gogtay N, Evans A, Rapoport J, Giedd J (2006): Intellectual ability and cortical development in children and adolescents. Nature, 440:676-9.

Smith A, Goffman L, Sasisekaran J, Weber-Fox C (2012): Language and motor abilities of preschool children who stutter: evidence from behavioral and kinematic indices of nonword repetition performance. Journal of fluency disorders, 37:344-58.

Smith A, Sadagopan N, Walsh B, Weber-Fox C (2010): Increasing phonological complexity reveals heightened instability in inter-articulatory coordination in adults who stutter. Journal of fluency disorders, 35:1-18.

Smith SM, Jenkinson M, Johansen-Berg H, Rueckert D, Nichols TE, Mackay CE, Watkins KE, Ciccarelli O, Cader MZ, Matthews PM, Behrens TE (2006): Tract-based spatial statistics: voxelwise analysis of multi-subject diffusion data. NeuroImage, 31:1487-505.

Sommer M, Koch MA, Paulus W, Weiller C, Buchel C (2002): Disconnection of speech-relevant brain areas in persistent developmental stuttering. Lancet, 360:380-3.

Taylor JG, Taylor NR (2000): Analysis of recurrent cortico-basal ganglia-thalamic loops for working memory. Biological cybernetics, 82:415-32.

Thomalla G, Siebner HR, Jonas M, Baumer T, Biermann-Ruben K, Hummel F, Gerloff C, Muller-Vahl K, Schnitzler A, Orth M, Munchau A (2009): Structural changes in the somatosensory system correlate with tic severity in Gilles de la Tourette syndrome. Brain : a journal of neurology, 132:765-77.

Tourville JA, Guenther FH (2011): The DIVA model: A neural theory of speech acquisition and production. Language and cognitive processes, 26:952-981.

Verbeke G, Molenberghs G (2009): Linear mixed models for longitudinal data. Springer Science & Business Media.

Voytek B, Knight RT (2010): Prefrontal cortex and basal ganglia contributions to visual working memory. Proceedings of the National Academy of Sciences of the United States of America, 107:18167-72.

Walsh B, Mettel KM, Smith A (2015): Speech motor planning and execution deficits in early childhood stuttering. Journal of neurodevelopmental disorders, 7:27.

Wang R, Benner T, Sorensen AG, Wedeen VJ (2007): Diffusion toolkit: a software package for diffusion imaging data processing and tractography. InProc Intl Soc Mag Reson Med, Vol. 15, No. 3720.

Watkins KE, Smith SM, Davis S, Howell P (2008): Structural and functional abnormalities of the motor system in developmental stuttering. Brain : a journal of neurology, 131:50-9.

Wechsler D (1999): Wechsler abbreviated scale of intelligence. Psychological Corporation.

Wechsler D (2002): Primary Scale of Intelligence–III. San Antonio: Psychological Corporation.

Williams KT (2007): EVT-2: Expressive vocabulary test. Pearson Assessments.

Yairi E, Ambrose NG (1999): Early childhood stuttering I: persistency and recovery rates. Journal of speech, language, and hearing research : JSLHR, 42:1097-112.

Yairi E, Ambrose NG (2005): Early childhood stuttering for clinicians by clinicians. Austin, Tex. PRO-ED.

Yendiki A, Koldewyn K, Kakunoori S, Kanwisher N, Fischl B (2014): Spurious group differences due to head motion in a diffusion MRI study. NeuroImage, 88:79-90.

Yoon U, Fonov VS, Perusse D, Evans AC, Brain Development Cooperative G (2009): The effect of template choice on morphometric analysis of pediatric brain data. NeuroImage, 45:769-77.

Zalesky A (2011): Moderating registration misalignment in voxelwise comparisons of DTI data: a performance evaluation of skeleton projection. Magnetic resonance imaging, 29:111-25.

Zielinski BA, Prigge MB, Nielsen JA, Froehlich AL, Abildskov TJ, Anderson JS, Fletcher PT, Zygmunt KM, Travers BG, Lange N, Alexander AL, Bigler ED, Lainhart JE (2014): Longitudinal changes in cortical thickness in autism and typical development. Brain : a journal of neurology, 137:1799-812.

Table 1. Demographics and behavioral scores averaged across longitudinal visits for each participant.

	Controls, n=43 (21 boys)		Persistent, n=23 (16 boys)		Recovered, n=12 (6 boys)	
	Mean (SD)	Range	Mean (SD)	Range	Mean (SD)	Range
Age at scanning (years)	7.5 (2.0)	3.7-11.2	7.8 (2.3)	3.7-11.6	7.2 (1.9)	5.2-10.3
Interscan interval (years)	0.93 (0.25)	0.64-2.22	1.03 (0.21)	0.68-1.78	0.95 (0.16)	0.73-1.33
Average number of scans	2.4 (1.0)	1-4	2.4 (1.2)	1-4	3.1 (1.2)	1-4
SES[a]	6.3 (0.6)	5.0-7.0	6.0 (0.9)	4.0-7.0	6.4 (0.6)	5.5-7.0
IQ[a]	114.6 (14.4)	84.0-144.0	105.3 (16.6)[b]	81.0-138.0	103.6 (12.9)[c]	88.0-124.0
PPVT	118.8 (12.7)	93.5-141.3	108.8 (14.3)[b]	85.0-146.3	113.1 (12.0)	85.0-131.0
EVT	115.4 (11.4)	93.5-142.0	106.3 (12.5)[b]	85.0-138.0	107.6 (11.0)[c]	89.3-128.8
GFTA	104.7 (6.6)	87.0-115.3	101.6 (6.2)	87.0-113.0	106.7 (7.5)	90.5-113.5
SSI-4 at the initial visit	N/A	N/A	22.5 (8.0)	13.0-48.0	17.5 (5.4)	8.0-26.0
SSI-4 at the final visit	N/A	N/A	20.4 (10.5) [d]	9.0-48.0	9.1 (3.0)	4.0-15.0

[a] Tests measured only at each participant's initial visit
[b] Scores significantly lower in persistent than controls (two-sample t-tests, $p<0.05$)
[c] Scores significantly lower in recovered than controls (two-sample t-tests, $p<0.05$)
[d] Scores significantly higher in persistent than recovered (two-sample t-tests, $p<0.05$)
SD = standard deviation; SES = socioeconomic status; IQ = intelligent quotient; PPVT = Peabody Picture Vocabulary Test; EVT = Expressive Vocabulary Test; GFTA-2 = Goldman-Fristoe Test of Articulation; SSI-4 = Stuttering Severity Instrument Edition 4

Table 2. White matter regions showing significant group differences in the voxel-based analysis.

White matter tracts		Persistent < Controls			Persistent < Recovered			Recovered < Controls			Recovered < Persistent		
	L/R	x, y, z	max. t	mm^3	x, y, z	max. t	mm^3	x, y, z	max. t	mm^3	x, y, z	max. t	mm^3
Body of corpus callosum / cingulum	L	-14, 0, 34	3.78	331							-18, -40, 32	4.66	135
	R	14, 0, 32	3.88	162	16, -18, 42	4.63	118						
Body of corpus callosum (near SMA[a])	L							-14, -16, 56	4.36	135			
	R							22, -8, 50	5.59	392	16, -6, 52	4.83	216
Splenium of corpus callosum	L/R	-6, -36, 14	4.90	280	-4, -32, 16	4.50	165						
Arcuate fasciculus (parietal lobe)	L	-38, -46, 30	4.72	135				-42, -34, 30	4.95	213	-46, -32, 28	5.21	142
	R										40, -6, 24	5.28	125
Arcuate fasciculus (temporal lobe) / inferior longitudinal fasciculus	L	-42, -48, -4	4.39	162	-38, -52, -6	4.61	142	-38, -36, 8	5.50	314	-44, -40, 12	5.51	159
Cerebral peduncle (near thalamus)	L										-20, -22, -2	4.68	260
Cerebellar peduncle (cerebellum)	L				-18, -42, -40	3.93	138						
		Persistent > Controls											
Body of corpus callosum (near SMA)	R	20, -38, 52	5.15	162									

[a]SMA: Supplementary motor area

Table 3. White matter regions showing significant growth rate differences between groups (group by age interactions) in the voxel-based analysis.

White matter tracts		Persistent < Controls			Persistent < Recovered			Recovered < Controls			Recovered < Persistent		
	L/R	x, y, z	max. t	mm^3	x, y, z	max. t	mm^3	x, y, z	max. t	mm^3	x, y, z	max. t	mm^3
Body of corpus callosum / cingulum	L	12, -6, 30	4.91	145				-16, 18, 28	4.32	169			
	L	-18, -18, 36	5.40	118									
	L	-24, -32, 30	4.01	115									
	L	-16, 0, 32	5.61	111									
	R	22, -36, 36	4.31	233	8, -14, 38	4.60	135						
Body of corpus callosum (near SMA[a])	R	24, -14, 52	5.05	189	20, -20, 56	5.45	118						
Anterior thalamic radiation / forceps minor	L	-20, 24, 26	5.34	503							-18, 44, 4	4.84	179
	L	-22, 36, -6	5.27	135									
	R	14, 34, -8	5.18	189				14, 54, 14	5.62	246	14, 52, 14	7.03	226
Arcuate fasciculus (parietal part)	L	-36, -50, 26	4.56	263									
	R	34, -18, 24	4.73	142									
	R	30, -60, 18	4.66	118									
Arcuate fasciculus (temporal part)	L	-38, -38, 0	4.05	155									
/ inferior longitudinal fasciculus	L	-24, -24, -6	5.96	142									
Cerebral peduncle	L	-8, -20, -6	4.55	122									
	R	10, -38, -42	4.25	118									
Cerebellar peduncle	R	14, -70, -38	5.52	203	16, -60, -42	5.40	280						

Inferior longitudinal fasciculus (anterior temporal part)	R				40, 0, -30	5.28	138
Short frontal lobe tracts (near inferior frontal sulcus)	L				-30, 22, 36	4.51	138
		Persistent > Controls			**Recovered > Controls**		
Splenium of corpus callosum	L/R	0, -36, 16	5.30	152			
Body of corpus callosum (near SMA)	L				-18, -22, 52	4.29	132
	R				18, -22, 58	5.35	111
Cerebellar peduncle (cerebellum)	L				-24, -58, -34	6.57	149

[a]SMA: Supplementary motor area

Table 4. White matter areas exhibiting negative relation between FA and stuttering severity (SSI4 scores) in children with persistent stuttering.

White matter tracts	L/R	x, y, z	max. t	mm^3
Superior thalamic radiation	L	-26, 4, 32	-5.21	162
	R	28, 2, 28	-5.23	381
Anterior thalamic radiation / forceps minor	L	-28, 34, 14	-5.01	122

FIGURE CAPTIONS

Figure 1. FA reductions in children with persistent stuttering and children who recovered from stuttering relative to controls (group effect). (A-B) The left column shows the locations where significant FA reductions were found in the persistent group (blue) and the recovered group (green). Significant FA reductions in both persistent and recovered groups are indicated in red. The right column illustrates the white matter fibers passing through the regions showing FA reductions based on DTI tractography of a 9-year-old female control participant. (C) To illustrate the growth trajectories of each group, individual FA values in the clusters of FA reductions located in the left arcuate fasciculus and the mid body of the corpus callosum were plotted against age. White circles, blue squares and green triangles indicate individual FA values in the control, persistent and recovered groups respectively. Data points acquired from the same participant are connected by thin solid lines. The fixed effects of no interest including sex, IQ, and socioeconomic status were removed from the FA values. Linear trend lines were added to illustrate the developmental trajectories of FA in each group (controls: gray line, persistent: blue dashed line, and recovered: green dotted line). Abbreviations: arc-fp = arcuate fasciculus in the frontoparietal areas; arc-t = arcuate fasciculus in the temporal lobe; cc = corpus callosum; cg = cingulum; FA = fractional anisotropy; ilf = inferior longitudinal fasciculus; L.H. = left hemisphere

Figure 2. Reductions of FA growth rate in children with persistent stuttering and children who recovered from stuttering relative to controls (group by age interactions). (A-D) The left column shows the locations where significant lower FA growth rate were found in the persistent group

(blue) and the recovered group (green). Significant reductions of FA growth rate in both persistent and recovered groups are indicated in red. The right column illustrates the white matter fibers passing through the regions showing reductions of FA growth rate based on DTI tractography of a 9-year-old female control participant. (E) To illustrate the growth trajectories of each group, individual FA values in the speech-motor regions showing reductions of FA growth rate were plotted against age. White circles, blue squares and green triangles indicate individual FA values in the control, persistent and recovered groups respectively. Data points acquired form the same participant are connected by thin solid lines. The fixed effects of no interest including sex, IQ and socioeconomic status were removed from the FA values. Linear trend lines were added to illustrate the developmental trajectories of FA in each group (controls: gray line, persistent: blue dashed line, and recovered: green dotted line). Abbreviations: arc-fp = arcuate fasciculus in the frontoparietal areas; arc-t = arcuate fasciculus in the temporal lobe; atr = anterior thalamic radiation; cb = cerebral peduncle; cc = corpus callosum; cg = cingulum; FA = fractional anisotropy; fs = frontal lobe short fibers; ilf = inferior longitudinal fasciculus; L.H. = left hemisphere; str = superior thalamic radiation

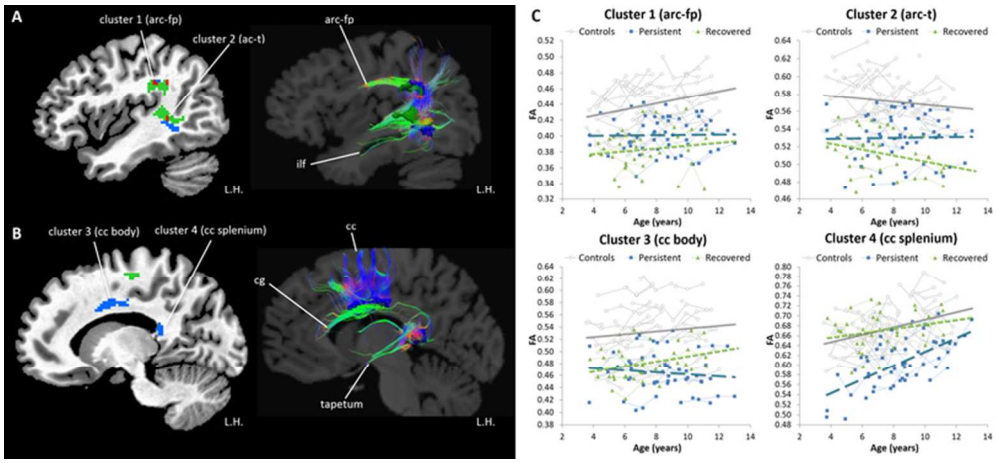

Figure 1. FA reductions in children with persistent stuttering and children who recovered from stuttering relative to controls (group effect). (A-B) The left column shows the locations where significant FA reductions were found in the persistent group (blue) and the recovered group (green). Significant FA reductions in both persistent and recovered groups are indicated in red. The right column illustrates the white matter fibers passing through the regions showing FA reductions based on DTI tractography of a 9-year-old female control participant. (C) To illustrate the growth trajectories of each group, individual FA values in the clusters of FA reductions located in the left arcuate fasciculus and the mid body of the corpus callosum were plotted against age. White circles, blue squares and green triangles indicate individual FA values in the control, persistent and recovered groups respectively. Data points acquired from the same participant are connected by thin solid lines. The fixed effects of no interest including sex, IQ, and socioeconomic status were removed from the FA values. Linear trend lines were added to illustrate the developmental trajectories of FA in each group (controls: gray line, persistent: blue dashed line, and recovered: green dotted line). Abbreviations: arc-fp = arcuate fasciculus in the frontoparietal areas; arc-t = arcuate fasciculus in the temporal lobe; cc = corpus callosum; cg = cingulum; FA = fractional anisotropy; ilf = inferior longitudinal fasciculus; L.H. = left hemisphere

69x31mm (300 x 300 DPI)

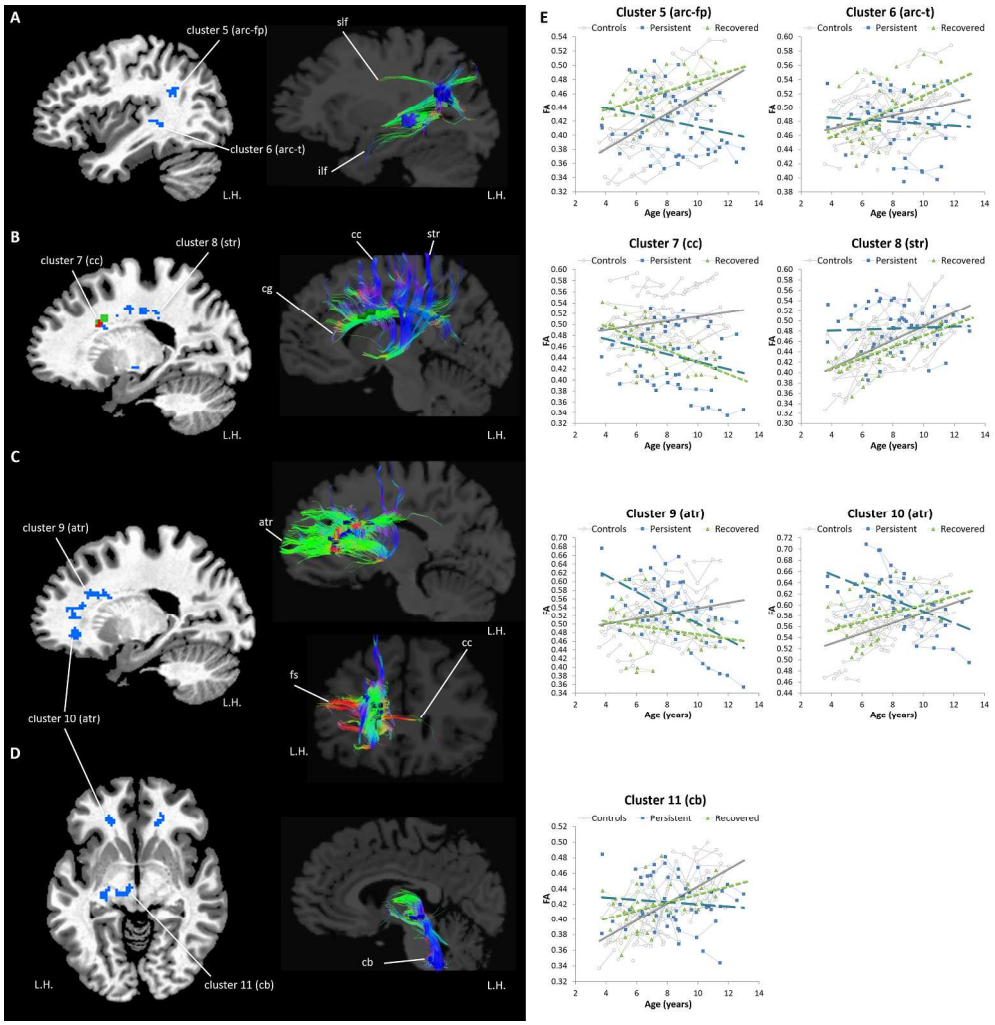

300x304mm (300 x 300 DPI)